General Disclaimer

One or more of the Following Statements may affect this Document

- This document has been reproduced from the best copy furnished by the organizational source. It is being released in the interest of making available as much information as possible.

- This document may contain data, which exceeds the sheet parameters. It was furnished in this condition by the organizational source and is the best copy available.

- This document may contain tone-on-tone or color graphs, charts and/or pictures, which have been reproduced in black and white.

- This document is paginated as submitted by the original source.

- Portions of this document are not fully legible due to the historical nature of some of the material. However, it is the best reproduction available from the original submission.

AgRISTARS

A Joint Program for Agriculture and Resources Inventory Surveys Through Aerospace Remote Sensing

Conservation and Pollution

THE CONTINUOUS SIMILARITY MODEL OF BULK SOIL-WATER EVAPORATION

ROGER B. CLAPP

REMOTE SENSING SYSTEMS LABORATORY
DEPARTMENT OF CIVIL ENGINEERING
UNIVERSITY OF MARYLAND
COLLEGE PARK, MARYLAND 20742

Lyndon B. Johnson Space Center
Houston, Texas 77058

TECHNICAL REPORT STANDARD TITLE PAGE

1. Report No.	2. Government Accession No.	3. Recipient's Catalog No.
CP-53-04417		

4. Title and Subtitle
The Continuous Similarity Model of Bulk Soil-Water Evaporation

5. Report Date
April 1983

6. Performing Organization Code

7. Author(s)
Clapp, Roger B.

8. Performing Organization Report No.

9. Performing Organization Name and Address
Remote Sensing Systems Laboratory
Department of Civil Engineering
University of Maryland
College Park, MD 20742

10. Work Unit No.

11. Contract or Grant No.

12. Sponsoring Agency Name and Address
USDA-ARS
Beltsville, MD 20705

13. Type of Report and Period Covered

14. Sponsoring Agency Code

15. Supplementary Notes

16. Abstract
See attached.

17. Key Words (Selected by Author(s))	18. Distribution Statement
Soil-water dynamics, evaporation, hydrological modeling.	UNLIMITED 43

19. Security Classif. (of this report)	20. Security Classif. (of this page)	21. No. of Pages	22. Price*
Unclassified	Unclassifed	50	

*For sale by the Clearinghouse for Federal Scientific and Technical Information, Springfield, Virginia 22151.

THE CONTINUOUS SIMILARITY MODEL OF BULK SOIL-WATER EVAPORATION

BY

Roger B. Clapp

ABSTRACT

In the past, evaporation from unvegetated soils has been simulated by using complex, numerical models of simultaneous moisture/heat flow and by using event models. The latter are attractive due to their relative simplicity although they have been difficult to apply to field conditions. This is so because variable climatic conditions and redistribution of soil water following infiltration both complicate the evaporation process.

Both factors are incorporated into the continuous similarity model of evaporation. In it, evaporation is conceptualized as a two-stage process. For an initially moist soil, evaporation is first climate-limited, but later it becomes soil-limited. During the latter stage, the evaporation rate is termed "evaporability," and mathematically it is inversely proportional to the evaporation deficit. In this relationship the model is similar to the Green-Ampt model of infiltration in which the infiltration rate is inversely proportional to cumulative infiltration. Unlike the Green-Ampt model, the evaporation model requires numerical integration. It also includes a functional approximation of the moisture distribution within the soil column.

The model was tested using data from 4 experiments conducted by the USDA-ARS near Phoenix, Arizona; and there was excellent agreement between the simulated and observed evaporation. The model also predicted the time of transition to the soil-limited stage reasonably well.

For one of the experiments, a third stage of evaporation, when vapor diffusion predominates, was observed. The occurrence of this stage was related

to the decrease in moisture at the surface of the soil. The continuous similarity model does not account for vapor flow.

The results of this study show that climate, through the potential evaporation rate, has a strong influence on the time of transition to the soil-limited stage. After this transition, however, bulk evaporation is independent of climate until the effects of vapor flow within the soil predominate.

TABLE OF CONTENTS

LIST OF TABLES

LIST OF FIGURES

PREFACE

This report is the sequel to a previous AgRISTARS publication entitled "The Desorptivity Model of Bulk Soil-Water Evaporation." As with the previous one, this report is not concerned with the mechanics of remote sensing, rather it deals with the physics of the near-surface region of the soil.

Of all the relationships developed herein, the item that may be most immediately helpful to the problem of interpreting moisture measurements obtainable by remote sensing is the functional approximation to the soil moisture profile described in Section 2. This approximation applies only when the soil surface is relatively dry, and it estimates the θ - z relationship only down to the zero-flux depth. Since this depth varies in time and rarely is expected to be greater than 50 cm, the approximation itself characterizes the difficulty in extrapolating the moisture distribution from surface measurements. Recognition of this difficulty reinforces the veiw point that simpler models -- like the one offered herein, and as opposed to complex, numerical ones -- offer the best avenue for infusing both soil physics and remote sensing into hydrological modeling.

Roger B. Clapp
March 1983

CHAPTER 1

INTRODUCTION

Physically based models of evaporation from unvegetated soils can be divided into essentially two groups: numerical models of simultaneous moisture/heat flow (e.g., Milly, 1982) and event models (e.g., Gardner and Hillel, 1962; Gardner et al., 1970 a,b). Models of the first group are complex and data-intensive, hence they are expensive to run and sometimes they give results that are difficult to interpret. The sheer volume of such results can possibly obscure simple mechanisms that can be controlling the evaporative process. In contrast, event models of evaporation are attractive due to their simplicity although their applicability is limited by their underlying assumptions and by the fact that they have never been satisfactorily field tested. Given these differences between models, it would be desirable to know what aspects of evaporation can be explained by a simple event model. From a practical standpoint, it is desirable to have a field-tested event model that could be merged with an infiltration model to yield a simplified, yet physically based model of the field water cycle. In turn, such a model could be applied to large-scale problems where the inherent uncertainties favor a simplified modeling approach.

Event models of evaporation simulate bulk flow, i.e., the rate of evaporation averaged over 24 hours; and they assume that evaporation can be divided into distinct stages. For an initially moist soil, the evaporation rate is mostly controlled by meteorological conditions. In time, a transition occurs when the rate becomes limited by the soil's ability to transport water to the near-surface region where evaporation actually occurs. The two intervals are identified as the climate-limited and the soil-limited stages, respectively, or simply as stages I and II.

As the soil becomes very dry there is a possibility of a third stage when evaporation is maintained at a low, and perhaps steady, rate by the diffusion of water vapor within the soil. Both the occurrence and the importance of stage-III evaproation under field conditions are open to question. In addition to these stages, Idso, et al. (1979) described a transitional interval between stages I and II when the soil surface exhibits both wet and dry areas. This "patichiness" is probably due to spatial variability in soil properties and/or microclimate. The model developed herein does not account for this variability or its effects on evaporation, although this phenomenon was observed in the experiments that provide the data used to test the model developed herein.

The fundamental assumption of event models is that stage-II evaporation is essentially independent of weather conditions. Nevertheless, it is common to see models that link stage-II evaporation to meteorological variables. For instance, Barton (1979) adapted the equation of Priestley and Taylor (1972) for potential evaporation to account for water loss from unsaturated surfaces; and Beese, et al. (1977) related the actual evaporation rate to the potential rate using an empriicism based on measures of soil-water-suction. Clearly, there is a basic contradiction between these approaches and the event models. For periods less than 24 hours, meteorological conditions are important in controlling evaporation because instantaneous rates of evaporation are correlated with net radiation, with the highest rates often occurring near solar noon. However, the focus of this research is on bulk evaporation, defined as the flux to the atmosphere averged over 24 hours. The question is whether bulk evaporation under field conditions can be adequately described by an event model.

This question was answered affirmatively in the previous paper (Clapp, 1983, henceforth referred to as Part I) in which stage-II evaporation was described by the desorptivity model. Despite its accuracy, that model has two significant drawbacks: one practical, the other conceptual. First, it requires an independent estimate of the time of transition to stage II. Although this time can be estimated *a posteriori* from changes in albedo, no predictive method was given. Second, the main equation of the model requires a fixed value for desorptivity, a key parameter in the model that is dependent on, among other things, the moisture content within the soil column. Due to the redistribution of moisture that follows infiltration, the moisture available for evaporation decreases in time so that the desorptivity also decreases. Consequently, the evaporation model includes an empirically chosen method for generating a representative value for desorptivity. The substitution of a physically based relationship for this empirical averaging technique would constitute an improvement.

1.1 Objectives

With these problems in mind, the first and second objectives of this paper are to describe and to test a model of bulk evaporation that estimates the time of transition and that incorporates the effect of redistribution directly. The new model, termed the Continuous Similarity Model (CSM), was tested using the same data used to develop the desorptivity model in Part I. The success of the model test provides more evidence that bulk evaporation during stage II is essentially an isothermal process. In other words, when evaporation is soil-limited the effects of temperature and energy on the rate of evaporation -- when averaged over 24 hours -- are negligible.

The model test also provides indirect evidence that the assumption of distinct stages is valid; but the ability to match cumulative evaporation over

a period of, say, 14 days does not prove the existence of separate stages. Consequently, the third objective is to examine the evaporation data directly to assess how distinct and identifiable the stages of evaporation are. Of prime importance is the occurrence of stage III when vapor flow predominates. Because the CSM does not account specifically for vapor diffusion, model errors in the calculated evaporation might occur under very dry conditions.

The fourth objective is to relate the observed stages of evaporation to the measured moisture content at the surface of the soil. Although the CSM does not require the surface moisture as an input, the surface moisture is important for a variety of reasons. For instance, it is strongly related to albedo and thus to the atmospheric energy budget. In addition, surface moisture can be measured indirectly by remote sensing; and it would be highly desirable to use such measurements to extrapolate the moisture profile, i.e., the moisture distribution with depth. Among other things, the CSM includes a functional approximation for the moisture profile (appropriate when the surface is relatively dry), and this expression may aid in the interpretation of remotely sensed data. It follows that the scope of this report ranges from the specific, conceptual development of the continuous similarity model to a broader investigation of the process of soil-water evaporation.

CHAPTER 2

MODEL DEVELOPMENT

The three main steps in the development of the continuous similarity model are presented in the next three sections. In the first section, the theoretical basis of the model, which was described in detail in Part I, is briefly reviewed. The fundamental expression for the rate of evaporation during stage II is introduced and then rearranged so that the rate is proportional to the reciprocal of the evaporation deficit, E*. This inverse relationship was first explored by Philip (1957), and in this form the evaporation model is analogous to the infiltration model of Green and Ampt (1911) in which the infiltration rate is inversely proportional to the cumulative infiltration. However, as is shown in the second section, E* in the CSM is not simply the cumulative evaporation. Although E* increases as evaporation continues, it is modified by the effects of redistribution. Quantification of the redistribution effect requires a functional approximation to the moisture profile, and this approximation is developed in the third section. Whereas the Green-Ampt model assumes a simple rectangular shape for the moisture profile, during evaporation the moisture profile is expected to be curved; this nonlinearity is critical to the estimation of the evaporation rate.

In the fully developed model, evaporation is described by the behavior of two dynamic state variables: E* and θ_1, the moisture content at depth. The temporal change in θ_1 results from the redistribution process which under certain circumstances can be assumed to be independent of evaporation.

In addition, the fully developed model has two special attributes. First, unlike the Green-Ampt model, the CSM requires numerical integration to advance the solution through time. Second, the CSM has two forms corresponding to the two commonly used expressions for soil-water diffusivity.

2.1 Desorption and the Evaporation Deficit

Part I describes the desorption problems of soil water dynamics and the associated "similarity solution." Together, these mathematical relationships provide the theoretical basis for the CSM. The desorption problem represents evaporation from a semi-infinite column of homogeneous soil having a uniform initial moisture content. The surface of the soil is assumed to be dried instantaneously and thereafter maintained at a low, steady moisture content. In addition, drainage effects are assumed to be negligible. At all times, the evaporation rate is soil-limited. In Part I, it was shown that the rate is sensitive to the soil's diffusivity function, as well as to the initial moisture content. However, it was also shown that the evaporation rate is largely indpendent of the surface moisture content provided that the moisture content is less than a critical value.

For the desorption problem the similarity solution is essentially a mathematical description of the moisture profile. For any diffusivity function, there is a unique function:

$$\theta(y) \quad \text{or} \quad \theta(z,t)$$

describing the moisture profile, where θ is the volumetric moisture content and y is the similarity variable defined by the relationship:

$$y = z(t - t_0)^{-1/2} \quad .$$

The parameter t_0 is an empirical time delay that accounts for the initial, climate-limited stage of evaporation; it is not included in the rigorous solution of the desorption problem. As shown in Part I, integration of the similarity moisture profile with respect to z yields the evaporation rate:

$$dE_2/dt = 1/2\ A(t - t_0)^{-1/2} \qquad (1)$$

which is the fundamental expression in the desorptivity model. In Eq. (1) E_2 refers to evaporation during stage II, and A is the desorptivity parameter which is functionally dependent on the moisture content at depth θ_1. The latter parameter is equivalent to the initial moisture content in the desorption problem; and in Part I, it was shown that θ_1 and therefore A decrease in time after the soil is initially moistened during infiltration. The change in θ_1 is caused by redistribution, and as mentioned before, this change has a significant effect on the evaporation rate.

In the past, analytical solutions for $\theta(y)$ and A were unavailable for commonly used diffusivity functions, but in Part I two approximations for A were presented. They were developed for two alternative expressions for diffusivity, specifically:

$$D_p = D_s(\theta/\theta_s)^{-c}$$

and

$$D_e = D_o \exp(a\theta)$$

referred to as power D and exponential D, respectively. The parameters D_s, D_o, c and a are usually fitted to D-θ data by regression, and there is no substantial evidence as to which expression for diffusivity is more appropriate. The approximations for A are

$$A_p = \left[\frac{12\, D_s \theta_s^{\,2}}{\pi (c+1)(c+4)} \left(\frac{\theta_1}{\theta_2}\right)^{c+2}\right]^{1/2} \tag{2}$$

for power D, and

$$A_e = \left[\frac{11.3\, D_o \theta_1 \exp(a\theta_1)}{a\pi (a\theta_1 + 1.85)}\right]^{1/2} \tag{3}$$

for exponential D. Both expressions are independent of the surface moisture content, θ_0, and they are considered to be accurate where $\theta_0 < \theta_c$, the critical moisture content (as defined in Part I).

In the new evaporation model, Eq. (1) for the evaporation rate is modified so that the independent variable t is eliminated, and the rate is calculated from the cumulative evaporation -- in much the same way as the infiltration rate in the Green-Ampt equation is calculated from the cumulative infiltration. To eliminate t, first (1) is integrated with respect to $(t - t_0)$:

$$E^* = A(t - t_0)^{1/2} \tag{4}$$

where E^* is the evaporation deficit. At this point, E^* is equivalent to the cumulative evaporation; however, a more general definition is given in the next section. Next, (4) is rearranged and substituted back into (1) to yield the expression:

$$dE_2/dt = (A^2/2)/E^* \tag{5}$$

which is merely a restatement of (1).

Under field conditions, the similarity solution cannot be applied rigorously because simultaneous redistribution decreases θ_1 through time. Despite this redistribuiton effect, the key supposition of the new model is

that (5) and a corresponding similarity moisture profile, $\theta(y)$, are continuously valid through stage II, hence the name "continuous similarity model." For simultaneous redistribution (5) is more appropriate than (1) because (5) relates dE_2/dt to the instantaneous distribution of the moisture within the soil column when the value of A in (5) is the instantaneous value. On the other hand, A in (1) must be fixed, so when redistribution changes θ_1 a time-averaged A must be specified. There is no physical basis for any particular averaging scheme.

For simplicity, (5) can be rewrtten as

$$dE_2/dt = \Phi(\theta_1)/E^* \tag{6}$$

where $\Phi = A^2/2$ and Φ is functionally dependent on θ_1. From (2) and (3) it follows that the approximations for Φ are:

$$\Phi_p = \frac{6\, D_s \theta_s^2}{(c+1)(c+2)\pi} \left(\frac{\theta_1}{\theta_s} \right)^{c+2} \tag{7}$$

for power D, and

$$\Phi_e = \frac{5.65 D_o \theta_1 \exp(a\theta_1)}{a\pi(a\theta_1 + 1.85)} \tag{8}$$

for exponential D. Φ represents the capability of a homogenous soil to move liquid water to a dry surface. Because (7) and (8) are simply manipulations of the approximations for A, the critical moisture content still serves as a guideline indicating how dry the surface must be. Again, for $\theta_0 < \theta_c$ the evaporation rate determined from (6) using (7) or (8) is considered to be a good approximation to complex, numerical approximations of the original similarity solution. The effects of the surface moisture on the evaporation

rate are more fully explored in the discussion section. It is sufficient at this point to note that θ_c values tend to be quite large, certainly larger than "air-dry" values of θ.

2.2 Effects of Redistribution and Climate

Following infiltration, the wetting front continues downward due to gradients in both the matric suction and the gravitational potential. Because no moisture is supplied to the surface, the moisture content behind the front decreases. The rate of decrease, termed the redistribution rate is initially large but decreases through time. I hypothesize that E* is conditioned by redistribution, i.e., E* simultaneously increases due to evaporation loss at the surface and decreases due to redistribution, as illustrated by the definition sketch in Figure 1. From that figure, it can be seen that

$$E^* = \int_0^{z_d} (\theta_1 - \theta) dz \tag{9}$$

and that the rate of change of E* is given by the expression:

$$dE^*/dt = dE/dt + z_d(d\theta_1/dt) \tag{10}$$

where dE/dt is the actual evaporation rate, and z_d is termed the depth of drying. Technically, z_d is the depth to the zero-flux point within the soil column; but for simplicity, in the CSM z_d and θ_1 are specified at the point of maximum θ above the wetting front. It follows that z_d increases in time as evaporation removes water from progressively lower depths. The rate of redistribution, $d\theta_1/dt$, is inherently negative; thus the redistribution effect tends to decrease E*. From (10) it can be seen that if $d\theta_1/dt = 0$, as required for the rigorous similarity solution, then E* is equivalent to the cumulative evaporation.

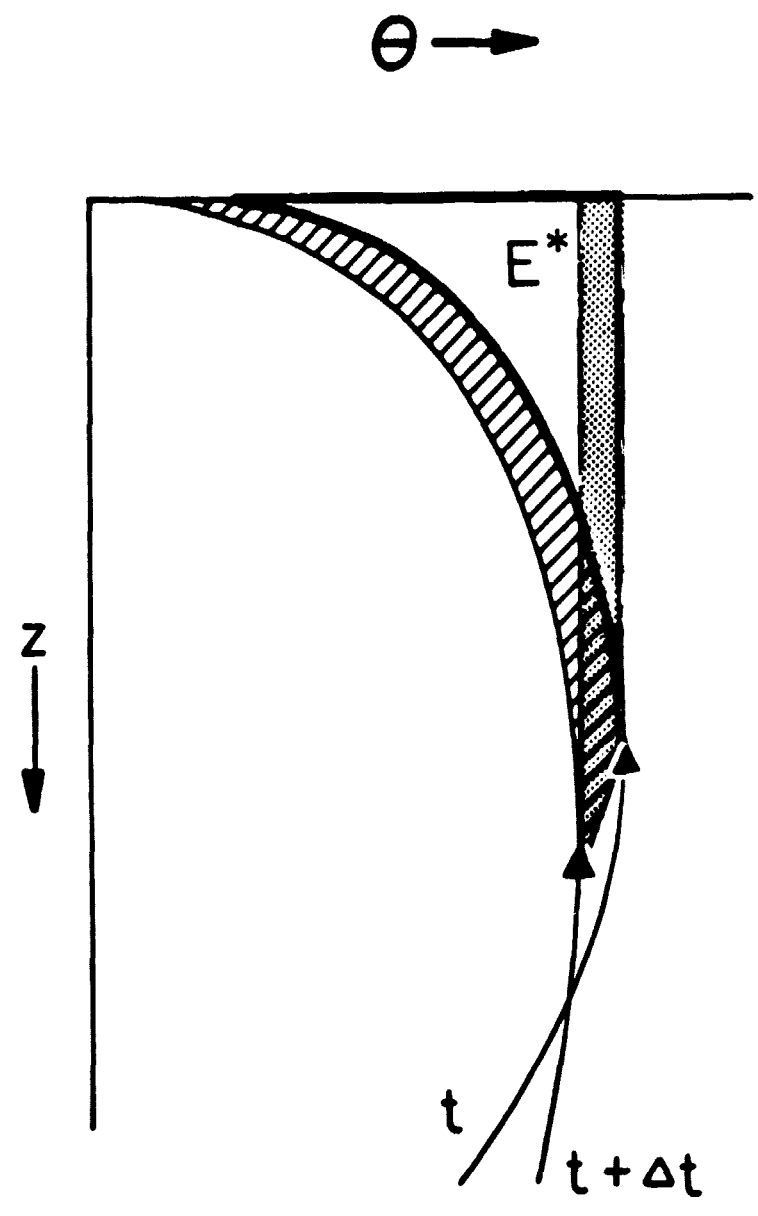

FIGURE 1. Definition sketch. For the CSM, E* corresponds to the area within the bold line. In time, E* is increased by evaporation (hatched area) and decreased by redistribution (gray area). The triangles indicate the depth of drying. Because the changes in E* due to evaporation and redistribution are evaluated continuously in the model, the overlap between the incremental changes shown in the diagram presents no problem.

To simulate evaporation as a two-stage process, the time of transition to stage II is computed implicitly. This is done by calculating dE_2/dt from (5) and by applying the following relationships:

$$dE_2/dt \geq PE \Rightarrow dE/dt = PE,$$

$$dE_2/dt < PE \Rightarrow dE/dt = dE_2/dt.$$

These relationships are analogous to those of Mein and Larson (1973) for determining the change from climate-limited to soil-limited infiltration. Hillel (1971) called the soil-limited rate of infiltration the soil's "infiltrability;" thus for the sake of symmetry, dE_2/dt is termed the soil's "evaporability." Evaporability serves to indicate both the beginning of stage II and the evaporation rate during stage II. Evaporability depends on E^*, and E^* is calculated from, among other things, the depth of drying. The estimation of z_d requires a mathematical expression for the moisture profile, and that is developed in the following section.

2.3 Moisture Profile

The specification of the moisture profile requires an alternative approximation to the similarity moisture profile. The alternative approach is based on the Kirchhoff transformation which was first applied to the process of soil-water evaporation by Gardner (1959). The transformation serves to simplify the governing equations for the desorption problem, and the reader is advised to compare the following equations with those of the original desorption problem in Part I. With the Kirchhoff transformation defined as

$$U = \int_{\theta_0}^{\theta} D\, d\theta \Big/ \int_{\theta_0}^{\theta_1} D\, d\theta \qquad (11)$$

and substituted into Eq. (1) of Part I, the partial differential equation for soil-water dynamics (without gravity flow) becomes

$$\frac{\partial U}{\partial t} = D(U) \frac{\partial^2 U}{\partial z^2} . \qquad (12)$$

With this transformation the initial and boundary conditions of the desorption problem become

$$t = 0,\ z > 0,\ U = 1$$

$$t > 0,\ z = 0,\ U = 0$$

$$t > 0,\ z \to \infty,\ U = 1.$$

From these transformed equations it is possible to derive simple functions for the moisture profile applicable whenever the surface is relatively dry.

Eq. (12) has an approximate solution:

$$U = \mathrm{erf}[z/(4\ D^{**}\ t)^{\frac{1}{2}}] \qquad (13)$$

where erf is the error function and D^{**} is an average diffusivity dependent on U. (Note that D^{**} is not readily related to the mean weighted diffusivity, D^{*}, of Part I.) In this solution, θ approaches θ_1 asymptotically so (13) does not computer a finite depth of drying. However, with two simplifying assumptions, (13) yields a useful approximation to both the moisture profile and z_d.

First, the error function is approximated by a simple linear function

$$\mathrm{erf}(X) = X$$

over the interval $0 \leq X \leq 1$. The reason for this approximation can be inferred from Figure 1 in Gardner (1959) which shows that the nonlinearity in the computed distribution is derived mostly from the transformation of the l.h.s. of (13) and not from the erf on the r.h.s.

Second, Eq. (12) for U can be simplified by assuming that $\theta_0 = 0$ and $\theta_c = -\infty$ for power D and exponential D, respectively. These substitutions make no appreciable difference to the calculation of bulk evaporation as shown in Part I. Hence, for power D, substitution into (13) yields

$$(\theta/\theta_1)^{c+1} = z/(4\ D^{**}\ t)^{\frac{1}{2}}$$

Because $z = z_d$ at $\theta = \theta_1$ the expression for the moisture profile is simply

$$(\theta/\theta_1)^{c+1} = z/z_d \tag{14}$$

The development of the moisture profile through time is reflected in z_d which is time-dependent. However, in the model z_d is not related directly to time but rather to E* which also increases in time. First, (14) is rearranged so that

$$\theta = \theta_1\ (z/z_d)^{1/(c+1)}.$$

Next, integration with respect to z from the surface to z_d and substitution of E* from (9) yields

$$z_d = (c+2)E^*/\theta_1. \tag{15}$$

For exponential D, the identical procedure yields

$$\exp[\alpha(\theta - \theta_1)] = z/z_d \tag{16}$$

and

$$z_d = \alpha E^*.$$

Through substitution into (6), the governing equation for the model is either

$$dE^*/dt = dE/dt + [(c+2)\ E^*\ d\theta_1/dt]/\theta_1 \tag{17}$$

or

$$dE^*/dt = dE/dt + a\, E^*\, d\theta_1/dt \qquad (18)$$

depending on the diffusivity function.

2.4 Model Overview

Either (17) or (18) serves as the rate equation for the state variable E^*. Another equation is needed for the other state variable θ_1, but in this study a simple, empirical expression is used. In the model test presented later, θ_1 is described by the power function:

$$\theta_1 = \hat{\theta}\, t^{-\beta}$$

and values for the parameters $\hat{\theta}$ and β are given in Part I. The form of the redistribution function is not critical, and Gardner, et al. (1970a) derived several functions from physical principals. It is assumed that redistribution is independent of evaporation, which is reasonable where antecedent infiltration is large; but the interaction between processes undoubtedly increases as antecedent infiltration decreases. This assumed independence is recognized as a possible source of error deserving further investigation.

Both (17) and (18) for dE^*/dt are complex; therefore E^* must be determined by numerical integration. Although the system is uniquely described by the temporal variation in E^* and θ_1, it is useful to integrate dE/dt to yield the cumulative evaporation, E. To generate the results reported in the next section, the rate equations for dE^*/dt and dE/dt were integrated using a second-order, Runge-Kutta routine with a 2-hr timestep. For exponential D, the required calculations to determine the rates are diagrammed in Figure 2. In the first

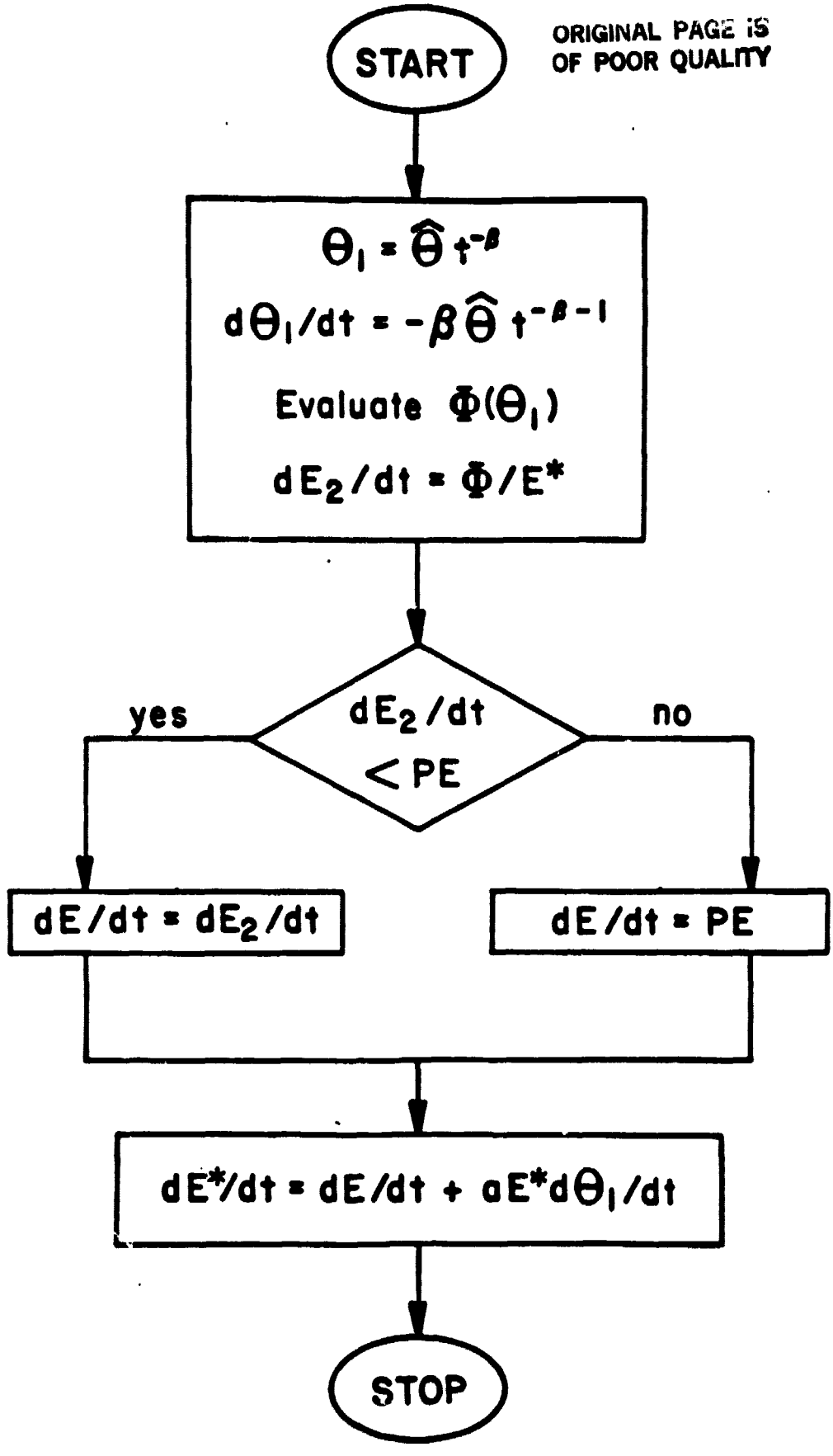

FIGURE 2. This procedure calculates the rate equations of the state variables; it is incorporated within the numerical integration scheme.

few hours of the simulation, dE^*/dt is negative and large in magnitude because the power function for θ_1 and its derivative are not valid. During this time, E^* is constrained to equal zero in the model. From a physical viewpoint, this constraint is reasonable because initially no appreciable near-surface deficit is formed. Instead the evaporative losses are distributed nearly uniformly with depth.

2.5 Comparison to the Infiltration Model

The model is now fully described, and the reader may choose to skip directly to the model test. However, it is enlightening to compare the basic equation for evaporability to the equation for infiltrability developed by Green and Ampt (1911). To do this, it is first necessary to describe their model.

For infiltration into a homogeneous soil having a uniform initial moisture content, θ_1, the infiltrability is given by

$$dI/dt = K_s(\theta_s - \theta_1)\ \psi_f/I + K_s \qquad (19)$$

where I is the cumulative infiltration, K_s is the hydraulic conductivity at saturation, and ψ_f is the wetting front suction. The water pressure at the surface is assumed to be zero. Neuman (1976) and others have derived (19) directly from Darcy's Law and in so doing, have defined ψ_f.

$$\psi_f = \int_{\psi(\theta_1)}^{\psi(\theta_s)} k\, d\psi$$

where k is the relative conductivity which is the ratio of unsaturated to saturated conductivities (K/K_s), and ψ is suction which is dependent on θ via the soil's characteristic curve. Because the integral is insensitive to $\psi(\theta_1)$, ψ_f is effectively constant for a given soil.

To transform the expression for evaporability into a form similar to (19) it is necessary to substitute expressions for ψ and K for diffusivity. This can be done using the relationships of Campbell (1974) for the moisture characteristic:

$$\psi = \psi_s(\theta/\theta_s)^{-b}$$

and for the conductivity function:

$$K = K_s(\theta/\theta_s)^{2b+3}$$

where ψ_s is the hypothetical ψ at θ_s. By applying the conventional transformation for D, Campbell's parameters can be related to the parameters in the expression for power D (as was done in Part 1). Similar relationships for exponential D are not available.

Using algebra and calculus it can be shown that

$$dE_2/dt = W K_s \theta_1 \psi_f(\theta_1)/E^* \qquad (30)$$

where W is a weighting factor, and ψ_f is now an "unsaturated wetting front suction" which is dependent on θ_1 via the expression

$$\psi_f = \int_0^{\psi(\theta_1)} k \, d\psi \, .$$

The integral is identical in form to that describing the saturated ψ_f.

A term-by-term comparison of expressions for evaporability and infiltrability indicates some of the inherent differences between the two processes. First, it is obvious that the constant flux term reflecting gravity flow during infiltration is dropped in the equation for evaporability (although drainage effects are calculated indirectly in CSM via the time-dependency of θ_1).

As for hydraulic conductivity, evaporability is related to K_s just as infiltrability is. At first glance, the inclusion of K_s is counterintuitive because the soil system is totally unsaturated during evaporation. This apparent inconsistency is resolved by noting that ψ_f is inversely proportional to K_s so that this factor is effectively canceled.

The expressions for both infiltrability and evaporability contain terms for the moisture deficit. This deficit indicates the pore space that is filled (infiltration) or depleted (evaporation) during the process. For infiltrability the term is $(\theta_s - \theta_1)$ whereas for evaporability it is simply θ_1. In essence, θ_1 is an effective moisture deficit during evaporation because (20) applies even when the surface is not completely dry (i.e., when $\theta_0 > 0$).

The insensitivity to surface conditions is more evident if (20) is rearranged so that the evaporation rate is inversely proportional to the depth of drying, instead of the evaporation deficit. Substitution of (15) into (20) yields

$$dE_2/dt = (c+2)\ W\ K_s\ [\psi_f(\theta_1)/z_d]. \qquad (21)$$

In this form, the moisture deficit has disappeared, and none of the remaining terms are dependent on the surface moisture.

Eq. (21) is analogous to the simplist form of the Green-Ampt model in which dI/dt is related to ψ_f divided by the depth of the wetting front. For both processes, the effect of suction is represented by the ψ_f, but the main difference is that for infiltration ψ_f is considered fixed for any soil type, whereas for evaporation ψ_f is dependent on θ_1. In (21) the evaporation rate is related to the averaged suction gradient, as represented by ψ_f/z_d. This relationship reflects the fact that bulk evaporation is affected by the moisture distribution in the whole zone of drying, from the surface down to z_d. This formulation contradicts the conventional wisdom that says that the evaporation rate is limited by a thin, dry, highly resistant layer at the surface.

The mathematical manipulations using Campbell's parameters which yielded (20) also yield an explicit expression for the W factor:

$$W = 6/[(c+4)\pi].$$

This weighting factor reflects the fundamental fact that desorption is inherently slower than sorption. Gardner (1959) arrived at the same conclusion based on his comparison of the mean weighted diffusivity for the two processes.

Future research may show that the concepts behind the Green-Ampt model may actually be more appropriate to evaporation than to infiltration. Of course, such a statement is mostly speculative; but for infiltration there are a variety of problems associated with the fact -- or at least the assumption -- that the soil system is saturated. For instance, the effects of entrapped air lead to empirical adjustments to K_s and ψ_f in the Green-Ampt model. For unsaturated systems, no such adjustments would be necessary. Nevertheless, there

are problems specifically associated with evaporation, for instance, the effect of vapor diffusion. This problem is discussed following the model test reported next.

CHAPTER 3

MODEL VALIDATION

The CSM was tested using the same data used to develop the desorptivity model in Paper I. Those data came from a series of experiments conducted by the staff of the USDA Agricultural Research Service near Phoenix, Arizona; and they are described by Jackson (1973) and Jackson et al. (1976). In each experiment a test plot and a nearby lysimeter were intially irrigated with about 10 cm of water; thereafter evaporation was measured every half hour. The experiments were performed at different times of the year so that essentially only climatic conditions varied among the experiments. For the March experiment only, the moisture profile was measured regularly from samples gathered in the test plot. In testing the CSM, the average PE rate and the parameters of the redistribution function were evaluated directly from the data. Although this informaiton cannot be known a priori, its use allows a more specific test of the model. Moreover, predictive equations for these variables are available.

There is one important difference in the information used to develop the desorptivity model and that used to test the CSM. The desorptivity model requires an independent estimate of the time of transition which is used directly in the calculations. For the CSM, this variable was used only to determine the average PE rate from the measured evaporation. In addition, the PE rate for the December experiment used in this test was 2.6 mm day^{-1}, instead of 2.1 mm day^{-1} as listed in Paper I. The rate was revised because subsequent analysis of the measured evaporation, reported later, suggested that the transition to stage II occurred on the sixth day following irrigation, rather than on day 10 as reported by Idso et al. (1974).

3.1 Results

As shown in Figure 3 and Table 1, the CSM yielded excellent estimates of the bulk evaporation measured by the lysimeter. For all 4 experiments the largest error in E after 14 days was less than 5%. Definitive statements concerning the model's predictive accuracy are not justified because information normally not available a priori was used in the calculations. However, the agreement between model and measurement leads to the conclusion that after the transition to soil-limited evaporation, climatic factors -- wind, heat, temperature -- are unimportant to the determination of bulk evaporation. This conclusion was also reached using the desorptivity model in Part I, and it specifically applies to stage II of evaporation. However, as discussed later, this conclusion must be qualified somewhat because the effect of weather on stage-III evaporation is still uncertain.

With respect to the time of transition, the model was fairly accurate. For all 4 experiments the differences between the calculated and observed times were less than 24 hours; this level of accuracy is the best that can be expected since the CSM applies only to average daily conditions. Because diurnal variations are not simulated the model can predict a transition to the soil-limited stage during the night, as was the case for the experiments of September, March and December. Considered on an hour-by-hour basis, soil-water evaporation is driven mainly by solar radiation. Hence, in reality the transition occurs during the daytime when the available energy and the diurnal PE rate are greatest.

FIGURE 3. Calculated and measured evaporation. The circled symbols indicate data used to generate the average PE rate.

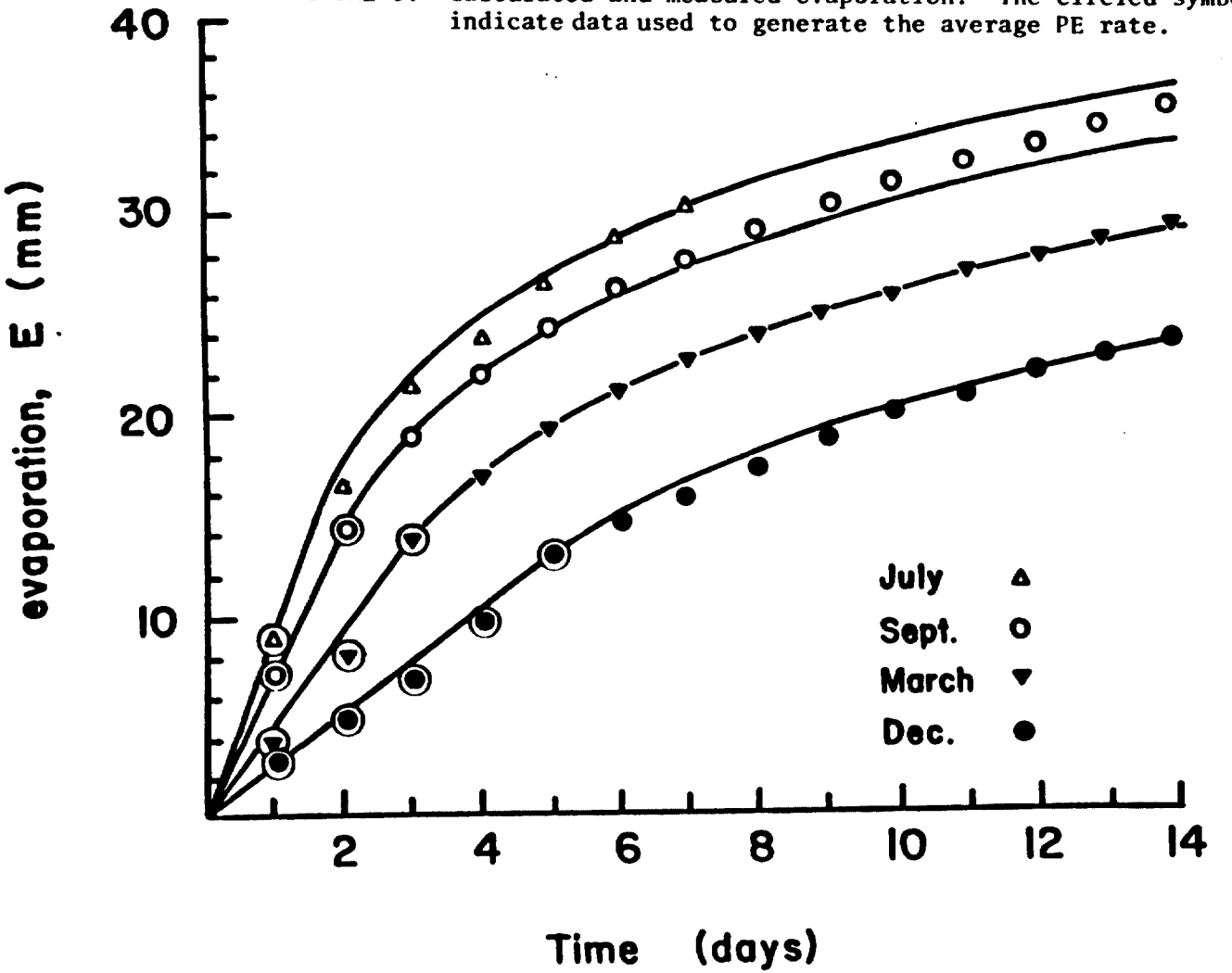

TABLE 1. Results from the Continuous Similarity Model

	End time	PE	Evaporation			Time to Transition		
			Calculated	Observed	Error	Calculated	Observed	Error
	(d)	(mm d^{-1})	(mm)	(mm)	%	(d)	(d)	%
July	7	9.1	30.2	30.6	-1.3	1.67	1.45	15
September	14	7.0	33.4	35.1	-4.8	2.08	2.46	-15
March	14	4.55	28.9	29.2	-1.0	3.02	3.39	-11
December	14	2.6	23.3	23.5	-0.9	5.00	5-6	0- -20

The results in Table 1 show that climate, through the PE rate, has a significant effect on the time of transition. Comparing two different climatic regimes and assuming other factors to be identical, the climate with the larger PE rate yields the earlier time of transition, as one would expect. But more importantly, the larger PE rate also yields the larger cumulative evaporation at all times, and the CSM predicts this pattern. It predicts this pattern even though the calculated evaporation is independent of PE after the transition, thus the results generated by the continuous similarity model lead to the same conclusions reached in Part I using the desorptivity model. The conclusion is that the conventional concepts of evaporation that lead to the practice of scaling actual evaporation rates to PE rates are unfounded from a physical basis; yet the result -- increased evaporation for increased PE rates -- is justified.

3.2 Calculated Moisture Profiles

For four selected days during the March experiment, the simulated profiles are plotted in Figure 4 along with soil moistures measured at noon on the respective days. For days 5, 9 and 14, the simulated profiles are consistantly drier than the actual profiles. This deviation conforms to the observations reported by Jackson, et al. (1976). They noted that for several days following the transition to stage II, the surface of the test plot was invariably wetter than that of the lysimeter. This is the problem of spatial variability that led Jackson, et al. (1976) to identify a transitional stage between the exclusively climate-limited and soil-limited stages. Because the focus of this test is to calculate the evaporative loss from the lysimeter, where the stage-I evaporation rates are precisely known, the discrepancies in Figure 4 for those 3 days are not considered to be important to this study.

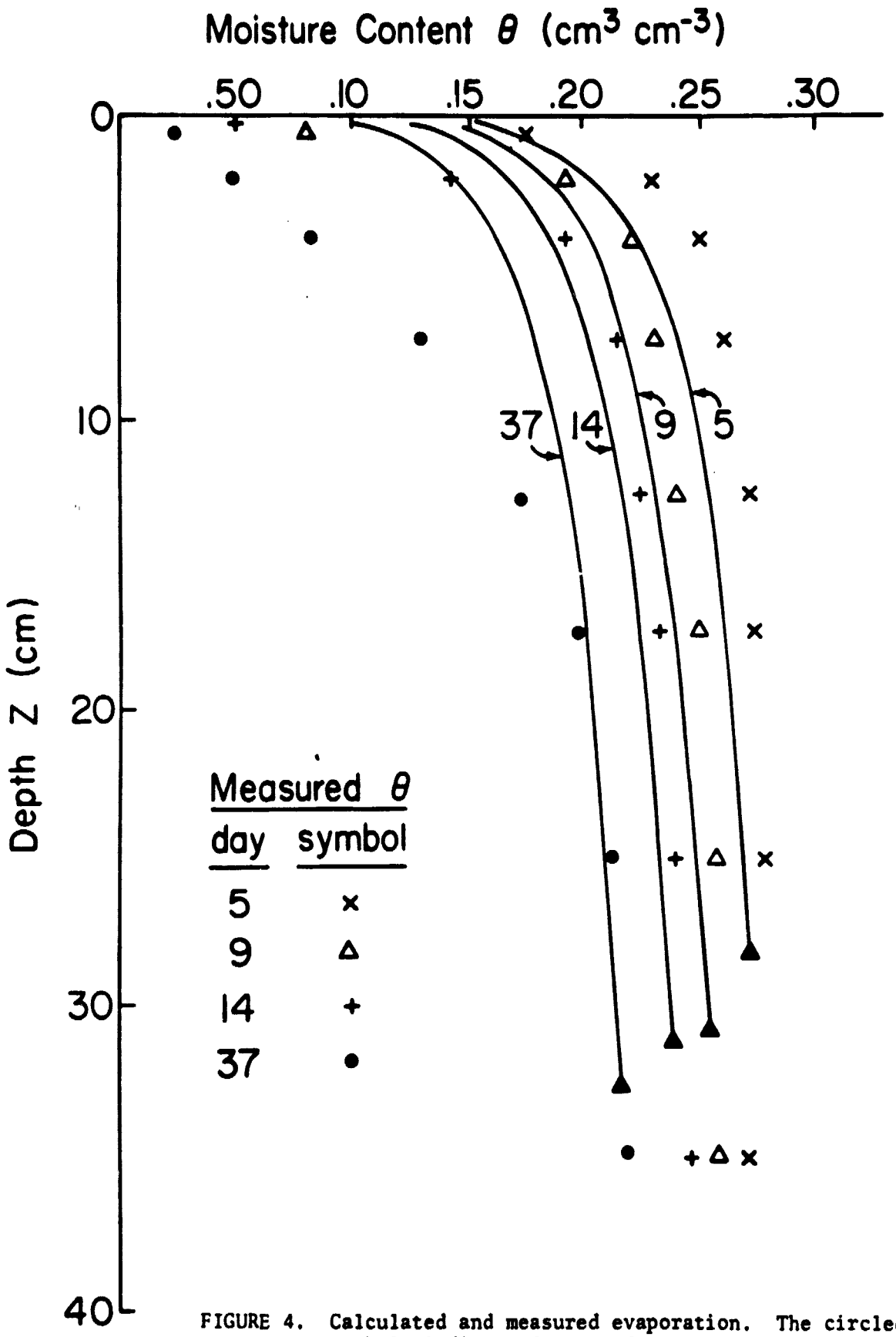

FIGURE 4. Calculated and measured evaporation. The circled symbols indicate data used to generate the average PE rate.

For the March experiment, additional measurements were made 15, 16, 23 and 37 days following irrigation. For day 37, there is a large difference in the simulated and observed profiles in Figure 4, and this difference is attributable to the vapor diffusion in the near-surface region that characterizes stage III. Vapor diffusion causes increased diffusivity at low θ, and theoretically, it results in a "drying front" or an inflection in the moisture profile (van Keulen and Hillel, 1974). Although this inflection point is not apparent in Figure 4, clearly neither the simple exponential diffusivity function nor the moisture profile function (Eq. 16) required by the CSM is applicable under these conditions. Consequently, it would be advantageous to know when the transition is likely to occur in order to evaluate the reliability of the model results. This problem is addressed in the discussion section.

The moisture profile is also described by the simulation variables E^* and z_d. In Figure 5, the computed E^* increases essentially linearly during stage I until the transition when the rate of increase diminishes and approaches zero. For all experiments, E^* is approximately 1/3 of the cumulative evaporation, E, the difference being caused by the redistribution effect. z_d is directly proportional to E^*, and it approaches 32 cm in all of the experiments.

As for the actual E^* for the March experiment, it is consistently less than the calculated value during the first two weeks, reflecting the tendency of the test plot to have a wetter surface than did the lysimeter. Late in the experiment the observed E^* becomes large due to vapor losses.

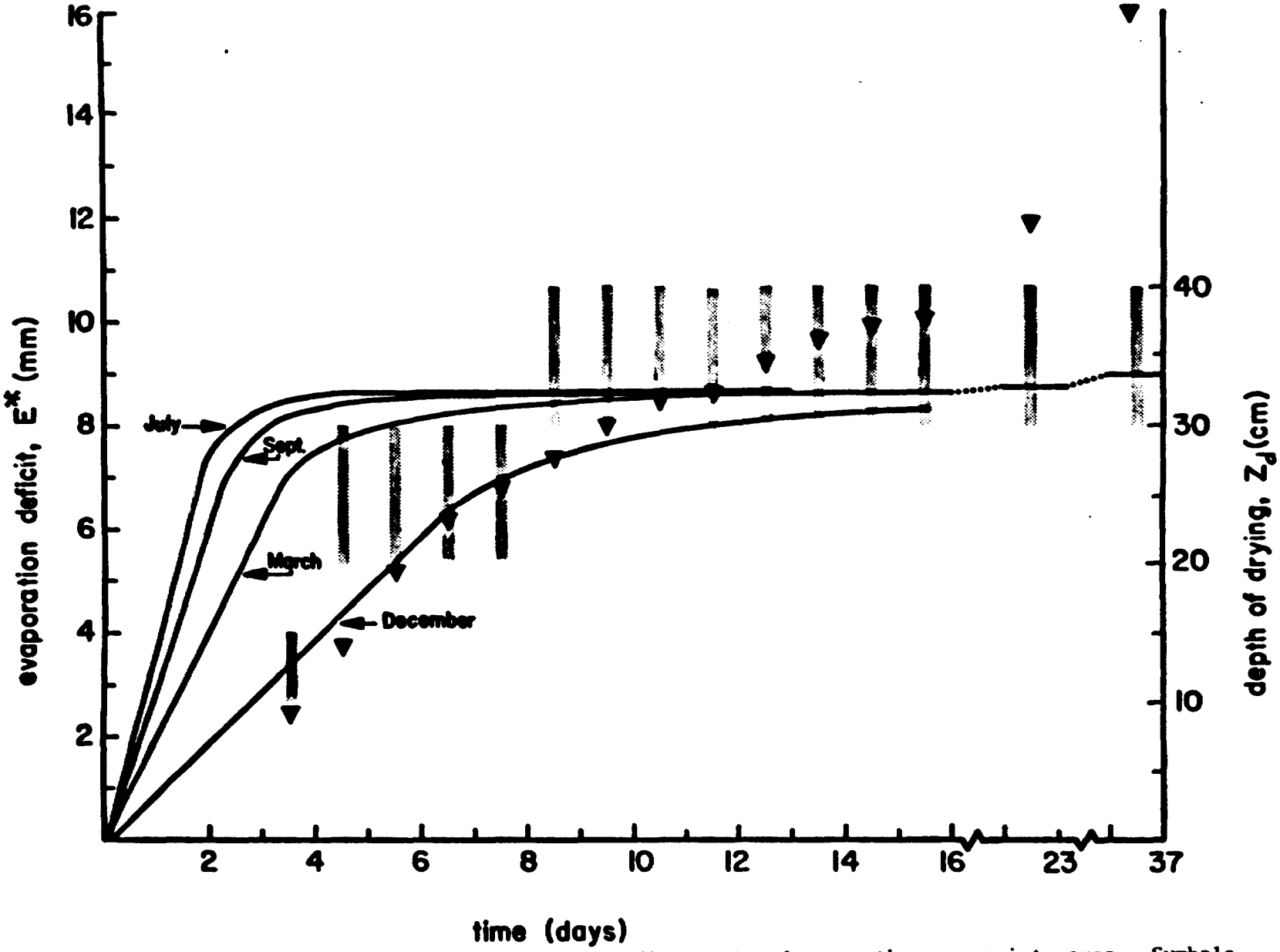

FIGURE 5. Model variables. The bold lines indicate E* and z_d on the appropriate axes. Symbols indicate the observed E* for March, and the hatched areas indicate the depth interval of maximum observed θ where the actual depth of drying probably occurred.

To illustrate the usefulness of the moisture profile function, the stored soil water, calculated and observed, are compared in Table 2. The stored water is calculated by integrating the moisture profile function (Eq. 16) between the surface and any selected depth, up to z_d. In Table 2, the depth of integration is limited by the increments of measurements of the actual moisture profile. To estimate the distribution of soil water stored below z_d, one needs a redistribution model to estimate the advance of the unsaturated wetting front. In Table 2, the computed results are reasonably accurate, but they do show the bias towards a dry profile relative to the field measurements during the first two weeks, followed by the reversed trend later due to vapor diffusion. The extrapolation of surface measurements to estimate soil water at deeper depths is a key problem in the development of remote sensing methods, and Eqs. (14) and (16) of CSM should prove useful.

TABLE 2. Water Stored Beneath the Surface

time	depth	calculated storage	observed storage	difference	error
(d)	(cm)	(mm)	(mm)	(mm)	%
3.67	10	22.6	25.8	-3.2	-12.4
4.67	20	47.0	50.9	-3.9	- 7.7
5.67	"	45.7	48.4	-2.7	- 5.6
6.67	"	44.7	46.6	-1.9	- 4.1
7.67	"	43.8	45.2	-1.4	- 3.1
8.67	30	67.9	69.8	-1.9	- 2.7
9.67	"	66.9	68.6	-1.7	- 2.5
10.67	"	66.1	67.3	-1.2	- 1.9
11.67	"	65.3	66.7	-1.4	- 2.1
12.67	"	64.6	65.6	-1.0	- 1.5
13.67	"	64.0	64.4	- .4	- .6
14.67	"	63.4	63.5	- .1	- .2
15.67	"	62.8	62.8	0.0	0.0
22.67	"	59.8	57.1	2.7	4.7
36.67	"	56.1	48.9	7.2	14.7

CHAPTER 4

DISCUSSION

At this point, the first two objectives of this report have been accomplished: the continuous similarity model has been fully described, and it has been tested. The discussion below addresses the remaining two objectives: to examine the evaporation data to see if they do indeed indicate the stages of evaporation, and to relate observed stages of evaporation to the measured surface moisture content. Note that the relationships observed below are more tentative than the results presented so far. This is so because there are very few data under very dry conditions, and because data from the lysimeter are related in this analysis to surface measurements made in the test plot, even though the previous section indicated discrepancies in these data sources. Nevertheless, the relationships are interesting enough to warrant examininations.

4.1 Stages of Evaporation

To examine the bulk evaporation, it is useful to consider the log-log transformation of dE/dt versus E. For the model results, this transformation is straightforward, yielding the continuous curves shown in Figure 6. For the field data, the hour-by-hour variation in the evaporation rate was eliminated by plotting the logarithms of each daily evaporative loss versus the cumulative loss at the end of that day.

For the March experiment, data for days 23 and 37 are also included although there is some uncertainty in the cumulative evaporation for those times. The cumulative amounts were determined by differencing the moisture

stored in the soil column and by assuming that no drainage occurred. The estimated range of error given this approximation is considerd to be negligible.

With respect to the simulated results shown in Figure 6, the transition between stages I and II is clearly depicted by the abrupt change in slope; and the field data also exhibit this abrupt change. In fact, the change in log dE/dt observed in the data between days 5 and 6 during the December experiment implies that stage II probably began sometime during day 6. This is the basis for adjusting the PE rate in the simulation. Additional, although indirect, evidence for a transition on day 6 is provided by the model itself which calculated the time of transition for the other three experiments.

As for the transition to stage III, only the data for the March experiment exhibit a new trend under very dry conditions. I interpret the deviations between the simulated and observed results for days 15, 16, 23 and 37 as stage-III evaporation. At the end of 37 days the actual evaporation is estimated to be about 50 mm, whereas the calculated amount is only 37 mm. Thus, the CSM is not applicable for prolonged periods of stage-III evaporation. Furthermore, the possible effects of climate on stage III are simply unknown.

As for the other experiments, I infer that the slight increases in log dE/dt for day 5 during July and for day 8 in September may result from stage-III condtions. This inference is based on the measurements in the surface moisture content described next. In any event, the bulk evaporation rates did not deviate much from the simulated results so there is no clear evidence of stage III during the July and September experiments.

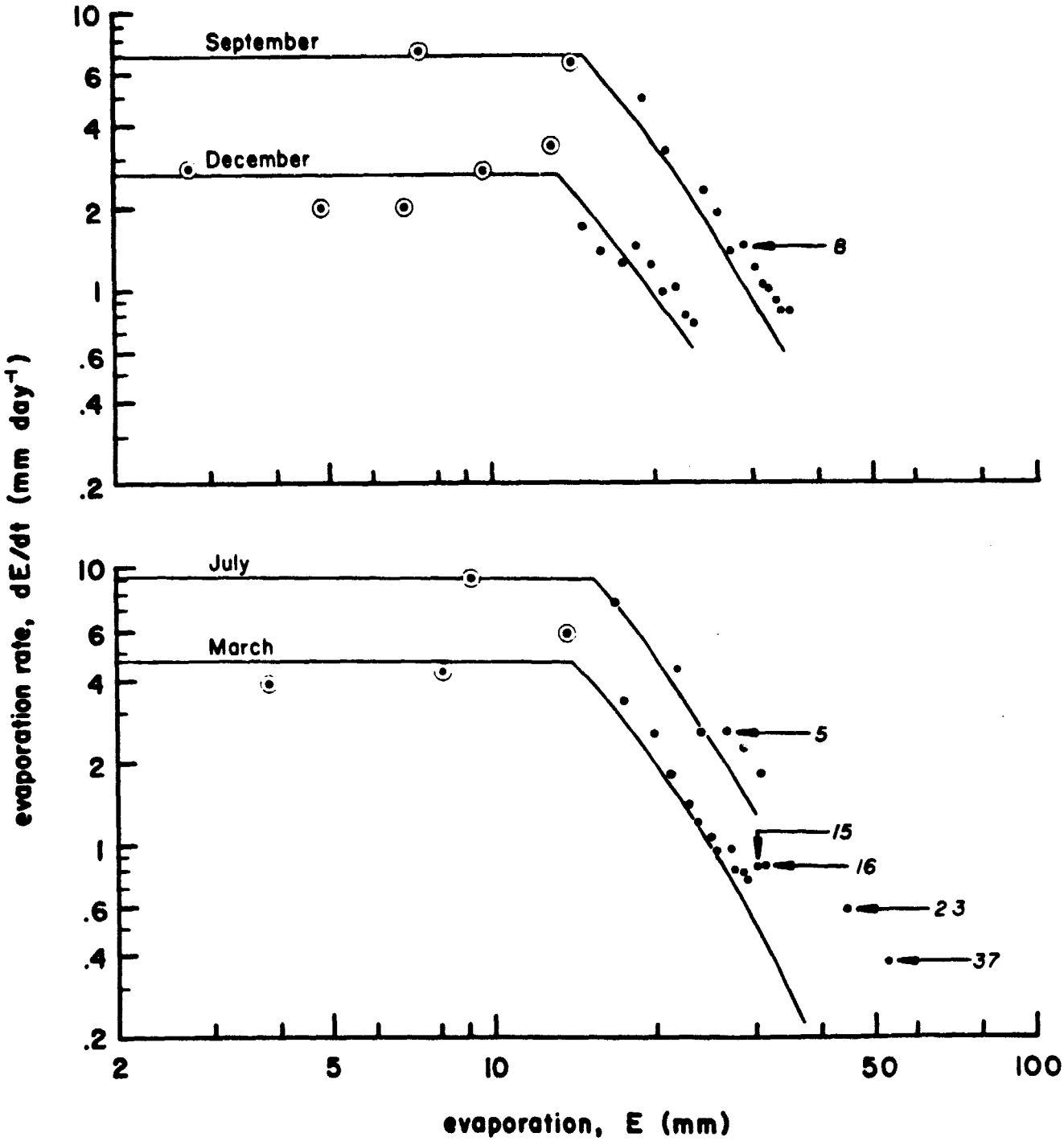

FIGURE 6. Transformed evaporation data. Each data symbol corresponds to one day, and certain symbols are individually identified by the number of days following irrigation. Simulated results for July, September, March, and December extend to 7, 14, 37 and 14 days, respectively. Circled symbols indicate data used to generate the average PE rates.

4.2 Surface Soil Moisture

Past researchers have stated that the surface moisture content can serve as an indicator of the different states of evaporation. For instance, Hillel (1971) stated that stage II begins when the surface is approximately air-dry. In contrast, Jackson (1973) stated that stage II begins when the surface has an intermediate wetness and that stage III begins when the surface is air-dry. With these conflicting views in mind, the purpose of this subsection is to relate the observed stages of evaporation to measurements of θ_0.

Continuous measurements of the near-surface moisture profile were made only during the July and March experiments. I investigated the average daily soil moisture, $\bar{\theta}_0$, and found trends in log $\bar{\theta}_0$ versus time that roughly correspond to the stages of evaporation identified above. For March, Figure 7 shows three linear trends in log $\bar{\theta}_0$, with the suggestion of a fourth one at the beginning of the experiment. Interestingly, the trends in log $\bar{\theta}_0$ are almost perfectly linear. The physical meaning for this linearity is unclear, but I am presently investigating these relationships.

In Figure 7, θ_0 is approximately .40 cm^3 cm^{-3} at t = 0, as extrapolated from deeper measurements. Assuming a straight-line trend, the first breakpoint in the data corresponds to the transition to stage II. In keeping with the observation of Jackson (1963), stage II begins when the surface has an intermediate $\bar{\theta}_0$. The second breakpoint occurs in the middle of stage II and corresponds to an average surface moisture of about .06 cm^3 cm^{-3} which is the air-dry value of θ for the particular soil, Avondale loam (Jackson, 1963). The break point probably signifies the beginning of intermittent vapor diffusion

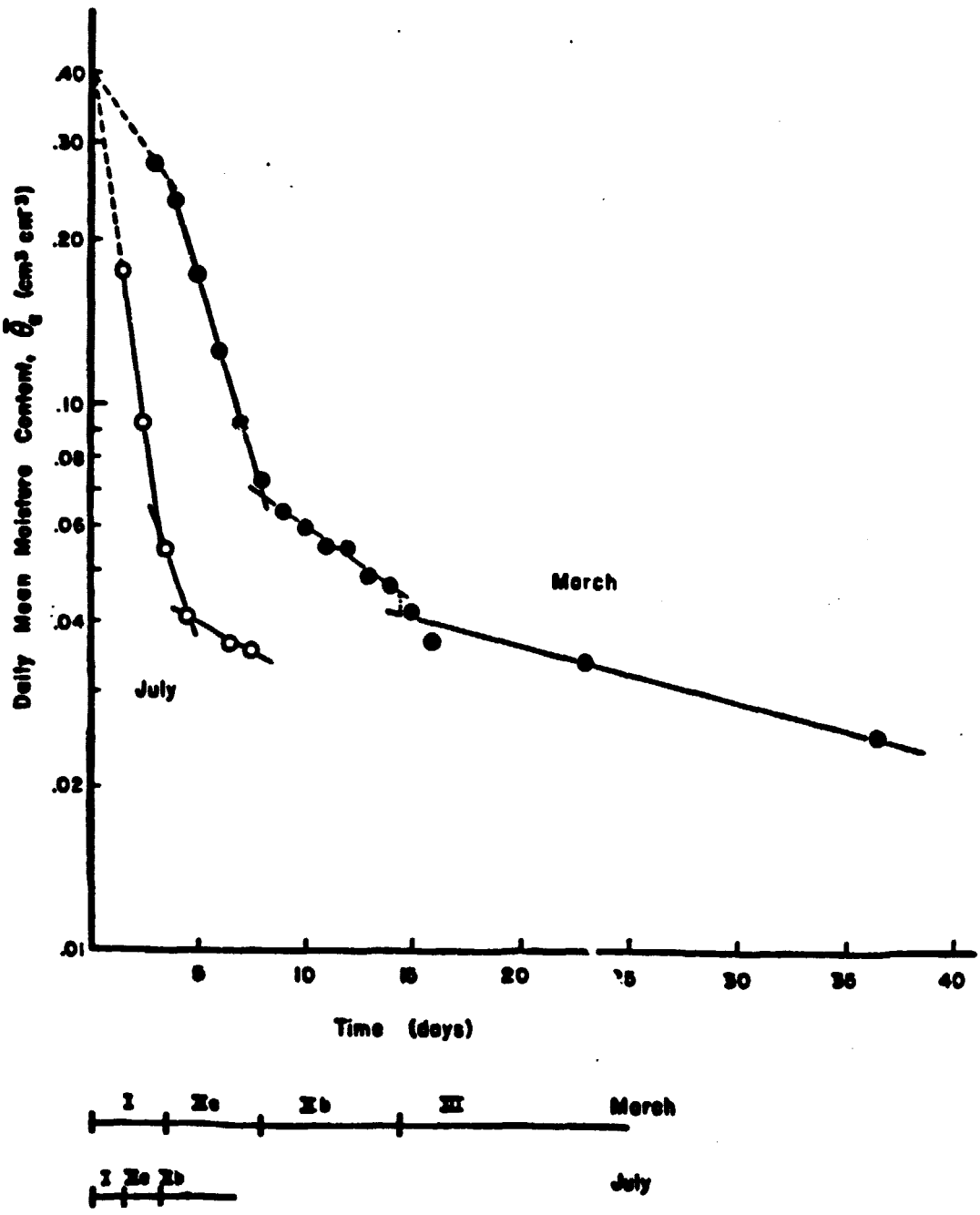

FIGURE 7. The daily average moisture content based on measurements from the uppermost 5-mm layer.

in the near-surface region, but there is no corresponding change in the evaporation rate. Thus, bulk evaporation is still limited by the movement of liquid water within the profile, and I have labeled this time interval as substage IIb. A third breakpoint occurs about day 14 when stage III began. In fact, day 14 is the first day when θ_0 remained less than air-dry throughout the day. Consequently, I conclude that stage III can commence when the surface remains less than air-dry throughout the entire day, and perhaps this "sub air-dry" condition could serve as a criterion for stage III.

There are few data for July, but based on the information for March, the same system of trends can be imposed on the data that are available. The data indicate that the surface became sub air-dry on day 5, much sooner than in March. However, there is no evidence of stage III in the evaporation data, so it appears that the soil surface may become sub air-dry while the evaporation rate declines in stage-II fashion. Therefore, a sub air-dry surface is a necessary, but not sufficient, condition for stage III; and it cannot be used as a sole criterion for stage III.

CHAPTER 5

CONCLUSIONS

Idike et al. (1977) demonstrated that infiltration under field conditions can be calculated from the minimal parameters required to describe the soil's hydraulic properties. Analogous to the Green-Ampt infiltration equation, the continuous similarity model describes evaporation from an unvegetated soil; and it, too, depends on fundamental hydraulic parameters. As demonstrated herein, the CSM is applicable under field conditions.

The fact that the model performed well in all 4 of the experiments tends to support the assumptions upon which the model is based. Based on the success of the simulations, it is concluded that for an initially moist soil, redistribution can be calculated independently of evaporation. Indeed, a submodel for redistribution must be incorporated if the CSM is to be a predictive model.

It is also concluded that bulk evaporation during stage II can be calculated without regard to the surface soil moisture. θ_0 does not affect dE/dt because of the nonlinearity of the fundamental hydraulic properties of soil. When θ_0 is moderately low the moisture gradient beneath the surface is steep. If θ_0 is decreased, the diffusivity decreases, but the gradient increases so that dE/dt remains virtually unchanged. Stated in a different manner, the soil water pores represented by the low range of θ never dry to any appreciable depth during stage II.

However, this conceptualization is not true during stage III, and it must be slightly modified when diurnal variations are considered, as was shown by Jackson (1963). With the daily pulses of sunlight, the surface layer also acts like a temporary storage compartment, discharging moisture during the day that accumulated from deeper with the profile during the night. However, the results reported here indicate that this storage effect does not control bulk evaporation. The controlling factor is the θ gradient between the surface and the depth of drying. In the model this gradient is represented by the state variables θ_1 and E^*, where E^* is directly related to the depth of drying.

This conceptualization differs with the often-stated viewpoint that evaporation is limited by a thin, dry, highly resistant layer at the surface. In fact, when the surface becomes air dry, its diffusive capability increases; and it can act as a wick, offering relatively little resistance to moisture moving upward from within the soil.

APPENDIX

COMPUTER CODE FOR THE CONTINUOUS SIMILARITY MODEL OF SOIL-WATER EVAPORATION

The FORTRAN program is listed on the next two pages, followed by a listing of the program's output. The program contains all the necessary information in the DATA statements, so input is not required. The parameters of the functions for diffusivity and redistribution are output using the NAMELIST convention. Subsequently, the simulation is completed four times, once for each of the seasonal experiments. The solution is obtained using a second-order, Runge Kutta integration method. The method requires that the rate equations for the evaporation deficit and cumulative evaporation (E^* and E, respectively) be evaluated twice at each time step. The rate equations are computed in the subroutine RATE which conforms to the flow chart given in Figure 2. The output, including values for the state variables and for their instantaneous rates, is printed for each day of the simulation.

```
C  CONTINUOUS SIMILARITY MODEL.
C*****************************************************************
C  PURPOSE-------    TO COMPUTE
C  BULK EVAPORATION AND THE EVAPORATION DEFICIT AS A
C  FUNCTION OF TIME.  REQUIRED INFORMATION INCLUDES A DIFFUSIVITY
C  FUNCTION, REDISTRIBUTION FUNCTION, AND INITIAL POT. EVAP. RATE.
C
C  IN THIS PROGRAM THE MODEL IS USED FOUR TIMES TO SIMULATE
C  THE FOUR DIFFERENT EXPERIMENTS IN THE PHOENIX DATA SET.
C  THE FOUR CASES REFER TO CONDITIONS IN JULY, SEPT., MARCH
C  AND DEC., RESPECTIVELY.
C
C*****************************************************************
C  GLOSSARY
C  DIFFUSIVITY FUNCTION-- D = DZERO * EXP (AL * THETA).  (MM**2/DAY)
C  REDISTRIBUTION FUNCTION-- THETA = THMAT * TIME ** BETA
C  THETA -- VOLUMETRIC MOISTURE CONTENT
C  PEV -- VECTOR OF 4 INITIAL POT. EVAP RATES (MM/DAY)
C  PE -- POT. EVAP. RATE (MM/DAY)
C  E--CUMULATIVE EVAPORATION (MM)
C  DEDT--EVAP. RATE (MM/DAY)
C  ESTAR--EVAP. DEFICIT (MM)
C  DESTDT-- RATE OF CHANGE OF ESTAR (MM/DAY)
C  DEOLD--PAST VALUE OF DEDT, USED TO DETERMINE THE TIME OF TRANS.
C  TMAX--END OF SIMULATION (14 DAYS)
C  DT--TIMESTEP (1/2 HOUR)
C  DTOUT--OUTPUT TIMESTEP (1 DAY)
C  PHI--BULK PARAMETER IN EVAPORABILITY EXPRESSION
C  ZD-- THE DEPTH OF DRYING.
C
C*****************************************************************
      COMMON /AA/DZERO,AL,THMAT,BETA
      COMMON/BB/DEOLD,THI,ZD,PE,DTHDT,DT
      DIMENSION PEV(4)
      NAMELIST/PARA/DZERO,AL,THMAT,BETA
      DATA DZERO,AL/.6048,.37,4/
      DATA PEV/9.1,7.0,4.55,2.6/
      DATA THMAT,BETA/.3216,.1102/
C
C  INITIALIZE TIME STEP PARAMETERS
      DT=.5/24.
      DTOUT=1.
      TMAX=14.
      WRITE(6,1000)
1000  FORMAT('1')
      WRITE(6,PARA)
C  REPEAT FOR EACH VALUE OF PE
      DO 500 JPE=1,4
      PE=PEV(JPE)
      TMAX=14.
C  INITIALIZE INTEGRATION VARIABLES.
      T=0.
      ESTAR=0.
      E=0.
      DEOLD=0.
      DESTDT=0.
      TOUT=DTOUT
      WRITE(6,1006)
 1006 FORMAT('0T',15X,'ERATE',9X,'E',8X,'ESRATE    ESTAR',
     1  9X,'ZD',10X,'THI')
C
C  SECOND ORDER INTEGRATION
C  FIRST EVALUATION OF RATE EQNS.
100   CALL RATE(DESDT2,DEDT2,ESTAR,E,T)
C  WORK ON INTERMEDIATE  VARIABLES TO ADVANCE INTEGRATION.
      ES2=ESTAR+DT*DESDT2
      E2=E+DT*DESDT2
      T=T+DT
      IF(T.GT.TMAX)GO TO 500
C
C  SECOND EVALUATION OF RATE EQNS.
          CALL RATE(DESTDT,DEDT,ES2,E2,T)
      ESTAR=ESTAR+DT*(DESTDT+DESDT2)/2.
      E=E+DT*(DEDT+DEDT2)/2.
C
      IF (T.LT.TOUT-.5*DT)GO TO 100
C  PRINT RESULTS
      TOUT=TOUT+DTOUT
      WRITE(6,1100)T,DEDT,E,DESTDT,ESTAR,ZD,THI
1100   FORMAT (' ',11F11.4)
      GO TO 100
C  END MAIN INTEGRATION LOOP: PROGRAM IS RECYCLED THRU 500 4 TIMES
500   CONTINUE
      END
```

```
      SUBROUTINE RATE(DESTDT,DEDT,ESTAR,E,T)
      COMMON/AA/DZERO,AL,THMAT,BETA
      COMMON/BB/DEOLD,TH1,ZD,PE,DTHDT,DT
C  THREE FUNCTIONAL STATEMENTS FOLLOW--
      THETA1(Z)=THMAT*Z**(-BETA)
      DTH1DT(W)=-BETA*THMAT*W**(-1.-BETA)
      PHI(W)=9.69*DZERO*W*EXP(AL*W)/(AL*3.1416*(AL*W+1.85))
C
      TH1=THETA1(T+1.E-10)
      IF(TH1.GT. .4)TH1=.4
C  THE MAIN EXPRESSION FOR EVAPORABILITY
      DEDT=PHI(TH1)/(ESTAR+1.E-10)
C
      IF(DEDT.GT.PE)DEDT=PE
      IF(DEOLD.EQ.PE .AND. DEDT.LT.PE)WRITE(6,1000)T,TH1,ZD
 1000 FORMAT (' TIME OF TRANSITION ',E17.8,' TH1 ZD',2F12.4)
      DEOLD=DEDT
      DTHDT=DTH1DT(T+1.E-10)
      ZD=AL*ESTAR
      DESTDT=DEDT+ZD*DTHDT

      IF(DESTDT.LT.0..AND. DEDT.LE.PE)DESTDT=0.
      END
```

$PARA D_0(mm^{2}day^{-1}) c ϕ θ
DZERO = .6048r000+000,AL = .37400000+002,THMAT = .3216000+000,BETA = .11020000+000
$END

T	(days)	ERATE (mm day^{-1})	E (mm)	ESRATE (mm day^{-1})	ESTAR (mm)	ZD (mm)	TH1 (cm^3 cm^{-3})
	1.0000	9.1000	9.1000	4.0485	3.0112	142.9356	.3216
TIME OF TRANSITION			1.6666664	TH1 ZD	.3040	241.9039	
	2.0000	6.2161	17.6141	1.6643	7.4126	277.2628	.2979
	3.0000	3.4570	22.1649	.2713	8.1383	304.3776	.2849
	4.0000	2.4244	25.0434	.0686	8.2495	309.7649	.2760
	5.0000	1.8704	27.1668	.0226	8.3280	311.2879	.2693
	6.0000	1.5231	28.6816	.0111	8.3385	311.8604	.2640
	7.0000	1.2848	30.2488	.0091	8.3483	312.2247	.2595
	8.0000	1.1111	31.4425	.0099	8.3577	312.5770	.2557
JULY	9.0000	.9768	32.4847	.0114	8.3683	312.9754	.2524
	10.0000	.8748	33.4095	.0129	8.3805	313.4311	.2495
	11.0000	.7909	34.2409	.0143	8.3941	313.9405	.2469
	12.0000	.7217	34.9961	.0154	8.4090	314.4957	.2446
	13.0000	.6638	35.6881	.0168	8.4248	315.0853	.2424
	14.0000	.6145	36.3265	.0170	8.4418	315.7107	.2404

T		ERATE	E	ESRATE	ESTAR	ZD	TH1
	1.0000	7.0000	7.0000	3.1142	2.9317	109.6428	.3216
	2.0000	7.0000	14.0000	3.2436	6.1179	226.8098	.2979
TIME OF TRANSITION			2.0833329	TH1 ZD	.2966	236.3993	
	3.0000	5.6462	19.0485	.6258	7.7189	286.3837	.2849
	4.0000	2.4876	22.0379	.1918	8.0719	301.8914	.2761
	5.0000	1.8992	24.2042	.0744	8.1967	306.9585	.2693
	6.0000	1.5387	25.9104	.0419	8.2548	309.7116	.2640
	7.0000	1.2941	27.3196	.0277	8.2880	309.9796	.2595
	8.0000	1.1171	28.5209	.0219	8.3124	310.8845	.2557
	9.0000	.9830	29.5651	.0196	8.3330	311.6553	.2524
SEPTEMBER	10.0000	.8778	30.4964	.0188	8.3522	312.3715	.2495
	11.0000	.7931	31.3304	.0186	8.3709	313.0703	.2469
	12.0000	.7234	32.0875	.0187	8.3895	313.7676	.2446
	13.0000	.6651	32.7809	.0189	8.4083	314.4695	.2424
	14.0000	.6155	33.4206	.0190	8.4272	315.1779	.2404

T		ERATE	E	ESRATE	ESTAR	ZD	TH1
	1.0000	4.9500	4.9500	2.0242	1.9056	71.2676	.3216
	2.0000	4.9500	9.1000	2.1084	3.9767	148.7244	.2979
	3.0000	4.9500	13.6500	2.1578	6.1114	228.5645	.2849
TIME OF TRANSITION			3.0208320	TH1 ZD	.2[illegible]7	228.5648	
	4.0000	2.7398	17.1346	.6539	7.2310	274.1832	.2760
	5.0000	2.0051	19.4654	.2815	7.7[illegible]7	290.3634	.2693
	6.0000	1.5938	21.2483	.1488	7.9689	296.0391	.2640
	7.0000	1.3266	22.7000	.0911	8.0853	302.3898	.2595
	8.0000	1.1379	23.9273	.0627	8.1606	305.2804	.2557
	9.0000	.9971	24.9916	.0474	8.2150	307.2402	.2524
MARCH	10.0000	.8878	25.9519	.0396	8.2576	308.8343	.2495
	11.0000	.8005	26.7745	.0332	8.2938	310.1693	.2469
	12.0000	.7290	27.5301	.0298	8.3247	311.3426	.2446
	13.0000	.6695	28.2368	.0278	8.3532	312.4103	.2424
	14.0000	.6190	28.8800	.0249	8.3798	313.4058	.2404

T		ERATE	E	ESRATE	ESTAR	ZD	TH1
	1.0000	2.6000	2.6000	1.1567	1.0669	40.7245	.3216
	2.0000	2.6000	5.2000	1.2048	2.2724	84.9865	.2979
	3.0000	2.6000	7.8000	1.2330	3.4922	130.6085	.2849
	4.0000	2.6000	10.4000	1.2531	4.7357	177.1155	.2760
TIME OF TRANSITION			4.9999967	TH1 ZD	.2693	223.2938	
	5.0000	2.5959	12.9999	1.2648	5.9948	224.2828	.2693
	6.0000	1.8483	15.1717	.6023	6.8716	256.9994	.2640
	7.0000	1.4638	16.6109	.3440	7.3276	274.0539	.2595
	8.0000	1.2214	18.1454	.2197	7.6027	284.3433	.2557
	9.0000	1.0521	19.2777	.1521	7.7858	291.1780	.2524
DECEMBER	10.0000	.9261	20.2639	.1121	7.9159	296.0541	.2495
	11.0000	.8283	21.1592	.0869	8.0148	299.7416	.2469
	12.0000	.7499	21.9270	.0702	8.0925	302.6582	.2446
	13.0000	.6856	22.6438	.0587	8.1566	305.0962	.2424
	14.0000	.6318	23.3017	.0505	8.2118	307.0912	.2404

ACKNOWLEDGEMENTS

Most of this research was funded by the U.S. Army Research Office. During the preparation of the manuscript, I have been supported by the Remote Sensing Systems Laboratory of the Department of Civil Engineering, University of Maryland.

REFERENCES

Barton, I.J., A parameterization of the evaporation from nonsaturated surfaces, J. Appl. Meteor., 18, 43-47, 1979.

Beese, F., R.R. Van der Ploeg, and W. Richter, Test of a soil water model under field conditions, Soil Sci. Soc. Amer. J., 41, 979-983, 1977.

Campbell, G.S., A simple method for determining unsaturated conductivity from moisture retention data, Soil Sci., 117, 311-314, 1974.

Clapp, R.B., The desorptivity model of bulk soil-water evaporation. AgRISTARS Report, 1983.

Gardner, W.R., Solutions of the flow equation for the drying of soils and other porous media, Soil. Sci. Soc. Amer. Proc., 23, 183-187, 1959.

Gardner, W.R., and D. Hillel, The relation of external evaporative conditions to the drying of soils, J. Geophys. Res., 67, 4319-4325, 1962.

Gardner, W.R., D. Hillel, and Y. Benyamini, Post irrigation movement of soil water: I. Redistribution, Water Resour. Res., 6, 851-861, 1970a.

Gardner, W.R., D. Hillel, and Y. Benyamini, Post irrigation movement of soil water: II. Simultaneous redistribution and evaporation, Water Resour. Res., 6, 1148-1153, 1970b.

Green, W.H., and C.A. Ampt, Studies in soil physics, I. Flow of air and water through soils, J. Agr. Sci., 4, 1-24, 1911.

Hillel, D., Soil Water: Physical Principles and Processes, Academic Press, New York, 288 pp., 1971.

Idike, F., C.L. Larson, D.C. Slack, and R.A. Young, Experimental evaluation of two infiltration equations, presentation to Amer. Soc. Agri. Eng., Annual meeting, Paper #77-2558, 1978.

Idso, S.B., R.J. Reginato, R.D. Jackson, B.A. Kimball, and F.S. Nakayama, The stages of drying of a field soil, Soil Sci. Soc. Amer. Proc., 38, 831-836, 1974.

Idso, S.B., R.J. Reginato, and R.D. Jackson, Calculations of evaporation during the three stages of soil drying, Water Resour. Res., 15, 487-488, 1979.

Jackson, R.D., Diurnal changes in soil water content during drying in Field Soil Water Regime, editied by R.R. Bruce et al., Spec. Publ. 5, 37-55 Soil Sci. Soc. Amer., Madison, Wis., 1973.

Jackson, R.D., S.B. Idso, and R.J. Reginato, Calculation of evaporation rates during the transition from energy-limiting to soil-limiting phases using albedo data, Water Resour. Res., 12, 23-26, 1976.

Mein, R.G., and C.L. Larson, Modeling infiltration during a steady rain, Water Resour. Res., 9, 384-394, 1973.

Milly, P.C.D., Moisture and heat transport in hysteretic, in homogeneous porous media: A matric head-bared formulation and a numerical model, Water Resour. Res., 18, 489-499, 1982.

Neuman, S.P., Wetting-front pressure head in the infiltration model of Green and Ampt, Water Resour. Res., 12, 564-566, 1976.

Philip, J.R., Evaporation and moisture and heat fields in soils, J. Meterol., 14, 354-366, 1957.

Priestley, C.H.B., and R.J. Taylor, On the assessment of surface heat flux and evaporation using large-scale parameters, Monthly Weath. Res., 100, 81-92, 1972.

van Keulen, H., and D. Hillel, A simulation study of the drying front phenomenon, Soil Sci., 118, 270-273, 1974.

*U.S. GOVERNMENT PRINTING OFFICE:1983-669-013/2406